Influence of viscosity on adipogenic and osteogenic differentiation of mesenchymal stem cells during 2D culture

Chengyu Lu [ab], Tianjiao Zeng [ab], Man Wang [ab], Toru Yoshitomi [a], Naoki Kawazoe [a], Yingnan Yang [c], and Guoping Chen [*ab]

[a] Research Center for Macromolecules and Biomaterials, National Institute for Materials Science, Ibaraki 305-0044, Japan.

[b] Graduate School of Science and Technology, University of Tsukuba, Ibaraki 305-8577, Japan.

[c] Graduate School of Life and Environment Science, University of Tsukuba, 1-1-1 Tennodai, Tsukuba, Ibaraki 305-8572, Japan.

[*] Correspondence: Guoping.CHEN@nims.go.jp; Tel: +81-29-860-4496

Keywords: viscosity, adipogenic differentiation, osteogenic differentiation, mesenchymal stem cells

Abstract

Accumulatively, cellular behaviours triggered by biochemical cues have been widely explored and the focus of research is gradually shifting to biophysical cues. Compared to physical parameters such as stiffness, substrate morphology and viscoelasticity, the influence of viscosity on cellular behaviours is relatively unexplored and overlooked. Thus, in this study, the influence of viscosity on the adipogenic and osteogenic differentiation of human mesenchymal stem cells (hMSCs) was investigated by adjusting the viscosity of the culture medium. Viscosity exhibited different effects on adipogenic and osteogenic differentiation of hMSCs during two-dimensional (2D) culture. High viscosity facilitated osteogenic while inhibiting adipogenic differentiation. During adipogenic differentiation, the effect of viscosity on cell proliferation was negligible. However, during osteogenic differentiation, high viscosity decreased cell proliferation. The different influence of viscosity could be explained by the activation of mechanotransduction regulators of Yes-associated protein (YAP) and β-catenin. High viscosity could promote YAP and β-catenin nuclear translocation during osteogenic differentiation, which was responsible for the increased osteogenesis. High viscosity inhibited adipogenesis through promoting YAP nuclear translocation. This study could broaden the understanding of how viscosity can affect stem cell differentiation during 2D culture, which is valuable for tissue engineering.

Introduction

Cells inhabiting tissues experience distinctive microenvironments and their functions can be modulated by both biochemical and biophysical cues [1–4]. As the solid effects of biochemical stimuli towards cells are gradually being verified, more and more studies have turned to biophysical cues such as stiffness, viscoelasticity, etc. [5–7]. Compared to physical parameters such as stiffness, viscoelasticity, ECM architecture and substrate curvature, the effect of viscosity on cell behaviours in particular the differentiation of stem cells is relatively unexplored.

Cells in physiological conditions are often surrounded by fluids of different viscosities. Extracellular fluids (ECF) are varied from different anatomical locations or when ageing, diseases or injury happens [8,9]. For example, the viscosity of interstitial fluid is around 3.5 cP [10]. The viscosity in mucus varies from 10,000 to 1,000,000 cP which is dependent on the different anatomical locations, ageing, diseases, etc. [11,12]. The viscosity of synovial fluid, which directly contacts articular cartilage, ranges from 4 to 40,000 cP [9,13]. The viscosity of the lipid within adipocytes is 36.8 cP [14]. The viscosity of bone marrow ranges from 37.5 to 400 cP [8]. To produce viscous microenvironments and enable mimicking physiological conditions, many naturally derived or synthesized materials have been employed. Maryam [15] took the merits of layer-by-layer coating and alginate to prepare viscous microcapsules and studied how shear stress affects stem cells' osteolineage commitment. Methylcellulose (MC), dextran, polyvinyl pyrrolidone (PVP) and polyethylene glycol (PEG) of different molecular weights and percentages have been used to control solution viscosities [16–18]. Besides these bioinert materials, bioactive materials such as gelatin have also been used in modulating viscosity [19–21].

However, most of these studies have focused on cancer cells. Elevated viscosity counterintuitively increases the motility of various cancer cells on 2D surfaces. Compared to the studies on cancer cells, studies of viscosity influence on normal cell functions are limited. Kyubae employed viscous gelatin for the three-dimensional (3D) culture of hMSCs and found that high viscosity increases alkaline phosphatase (ALP) activity, calcium deposition and osteogenesis-related gene expressions [21]. High viscosity is also beneficial for chondrogenesis while detrimental to adipogenesis in a 3D culture environment [19,21]. However, the viscosity in the study was only up to 175 cP, which is much lower than the physiological viscosity value.

Nevertheless, how physiological viscosity affects the differentiation of hMSCs population has received relatively little attention. Thus, in this study, the viscosity of cell culture medium at a large range simulating the viscous conditions of adipocytes and bone marrow was used for 2D culture and the influence of viscosity on proliferation and differentiation of hMSCs was investigated. To adjust medium viscosity, PEG was used because PEG is a bioinert material and provides an easier way to change viscosity by employing different molecular weights and percentages. Furthermore, the underlying mechanism of viscosity influence on stem cell differentiation was elucidated.

Materials and methods

Preparation of viscous culture medium

Polyethylene glycol (PEG) was employed to modulate medium viscosity due to its bioinert and biocompatible properties. The desired viscosities of high, low and middle were prepared by high molecular weight PEG (PEG 8M, Mw ~8,000,000, Sigma-Aldrich), low molecular weight PEG (PEG 35K, Mw ~35,000, Sigma-Aldrich) and their mixture at a weight ratio of 3:1, respectively. The polymers were firstly dissolved in Milli-Q water to prepare the stock solution of 1.5 w/v% and followed by passing through a Millipore syringe filter (0.22 or 0.45 μm, Merck Millipore) for sterilization. Concentrated Dulbecco's Modified Eagle's Medium-high glucose powder (H-DMEM, Sigma-Aldrich) and Dulbecco's Modified Eagle's Medium-low glucose powder (L-DMEM, Sigma-Aldrich) were used to prepare 10-times medium based on the company's protocol. Thereafter, 1.5% of the stock polymer solution was mixed with the concentrated DMEM medium supplemented with 10% fetal bovine serum (FBS, Gibco, CA, USA), 74 g/L sodium bicarbonate, 0.4 mM L-proline, 50 mg/L ascorbic acid, 100 U/ml penicillin and 100 μg/ml streptomycin to prepare the complete medium containing 1.0 w/v% polymers. The induction media were prepared according to the previous report [21]. For the viscous adipogenic medium, the complete H-DMEM was further supplemented with 1 μM dexamethasone (Dex, Sigma-Aldrich), 500 μM methyl-isobutylxanthine (IBMX, Sigma-Aldrich), 10 μg/ml insulin (Sigma-Aldrich) and 100 μM indomethacin (Sigma-Aldrich). For the viscous osteogenic medium, the complete L-DMEM was further supplemented with 0.01 μM dexamethasone and 1,000 μM β-glycerol 2-phosphate disodium salt hydrate (β-GP, Sigma-Aldrich). Induction medium without polymers was prepared in the same way as that mentioned above to serve as the normal viscosity group.

Viscosity and osmolarity measurement

MCR 302 rheometer (Anton Parr, Germany) was employed for the viscosity measurement using a rotational shear mode. The viscous solutions were placed between two parallel plates (PP-50) with a gap size of 1.0 mm and the measurement was performed under shear rates ranging from 0.1 to 100 /s at a constant temperature of 37 ℃. The viscosity at a shear rate of 0.1 /s was determined as the zero-shear viscosity. For the osmolarity measurement, a vapour pressure osmometer (Vapro 5600, Wescor ELITechGroup, Logan Utah, USA) was used and 10 μl was used for each measurement of quadruplicate samples.

Cell culture

Human bone marrow-derived mesenchymal stem cells at passage 2 (hMSCs, CAT. # PT-2501, LOT NO. 20TL262529, DONOR: 41229, POIETICS™) were subcultured to passage 4 and used in this study. A Falcon 24-well plate (Corning) was used to culture cells. Before cell culture, the plate was coated with fibronectin. Briefly, 200 μl of 20 μg/ml fibronectin solution (F0895-1MG, Sigma-Aldrich) in $NaHCO_3$ (pH = 8.4) was added into each well, then the plate was incubated at 37 ℃ for 1 h and followed by thoroughly washing with $NaHCO_3$ solution and Milli-Q water. Fibronectin antibody (sc-8422, Santa Cruz) combined with Alexa Fluor 488-labeled donkey anti-mouse lgG secondary antibody

(1:1000, A21202, Invitrogen) were used to visualize the coated fibronectin. The fibronectin-coated plates were seeded with 1 ml of hMSCs per well at a concentration of 50,000 cells/ml suspended in MSCGM (PT-3001, Lonza). After 1 d of culture in a 5% CO_2 incubator at 37 ℃, the complete medium was pipetted out and the corresponding viscous induction media (1 ml) were added into each well. The medium was refreshed every 3 d during the differentiation processes. The whole period of 21 d was scheduled for the adipogenic and osteogenic differentiation. During the differentiation processes, cell morphology was checked by an all-in-one microscope (BZ-X810, KEYENCE). Besides, for cytoskeleton visualization, 5,000 cells were seeded in each well instead. F-actin staining was performed on 0, 1, 3 and 7 d.

Cell viability, apoptosis and cell proliferation assay

Cell viability before the culture media were changed to the differentiation induction media and after 21 d culture in the induction media was checked with a cell double staining kit (CS01/341-07381, DOJINDO). The samples were incubated in a serum-free medium containing 2 μM of calcein-AM and 4 μM of propidium iodide at 37 ℃ for 15 min. After staining, the cells were observed by an all-in-one microscope (BZ-X810, KEYENCE).

To probe the effects of viscosity on hMSCs apoptosis during the differentiation period, TUNEL (terminal deoxynucleotidyl transferase-mediated dUTP nick-end labelling) staining was conducted on 7 d. Briefly, cells were washed with PBS twice followed by fixation with 4% paraformaldehyde/PBS (pH 7.4) at room temperature for 15 min. To improve the penetration of the enzyme reaction solution, 100 μl of permeabilization buffer (MK505, TaKaRa) was added for 5 min at 4 ℃. After washing with PBS twice, 100 μl of the reaction mixture which was prepared by mixing 10 μl TdT Enzyme (MK502, TaKaRa) and 90 μl Labeling Safe Buffer (MK501, TakaRa) was added to the sample and reacted for 90 min at 37 ℃. The stained cells were viewed by an all-in-one microscope (BZ-X810, KEYENCE).

For cell proliferation, DNA amount in each sample was measured after culture for 1 d post seeding and after culture in the induction media for 7 d, 14 d and 21 d. A DNA quantification kit (DNAQF-1KT, Sigma-Aldrich) was used to measure the DNA amount. Firstly, 500 μl of trypsin-EDTA solution (T4049-100 ml, Sigma-Aldrich) was added into each well after washing with PBS twice. Then, the cells were digested in an incubator for 5 min at 37 ℃. After snap freezing and freeze-drying, 500 μl of papain solution (400 μg/ml in 0.1 M phosphate buffer, pH 6.0, P4762, Sigma-Aldrich) supplemented with 5 mM ethylenediaminetetraacetic acid disodium salt dihydrate (E5134-100G, Sigma-Aldrich) and 5 mM L-cysteine hydrochloride monohydrate (C7880-100G, Sigma-Aldrich) was added. The samples were then incubated at 60 ℃ for 6 h with shaking. Finally, an aliquot of the papain digestion solution was mixed with bisbenzimide Hoechst 33258 and measured with an FP-8500 spectrofluorometer (JASCO, Japan) at excitation/emission 360/460 nm. DNA amount was calculated based on a standard fluorescence curve. Triplicate samples were used for the measurements (n = 3).

Adipogenesis-related staining and quantification

Oil Red O staining was performed to visualize the formation of lipid vacuoles for the evaluation of adipogenesis after hMSCs were cultured in the adipogenic induction media for 14 d. Specifically, the cells in the 24-well plate were rinsed with PBS thrice, followed by fixation with 4% paraformaldehyde phosphate buffer solution for 10 min at 4 ℃. Thereafter, the cells were washed with water thrice and soaked in 60% 2-propanol (166-04836, FUJIFILM Wako Pure Chemical Industries, Ltd.) for 5 min. After aspiration of the 60% 2-propanol, the cells were immersed in a 60% Oil Red O working solution for 10 min at room temperature. Oil Red O working solution was prepared by dissolving Oil Red O powder (O0625, Sigma-Aldrich) in 2-propanol and then mixed with Milli-Q water at a volume ratio of 3:2. Finally, the stained cells were washed with Milli-Q water thrice and observed under an optical microscope to capture phase-contrast photos. For quantification, the stained cells in each well were dried in the air and Oil Red O dye was extracted by adding 400 μl of 2-propanol at room temperature for 2 h. Then, 100 μl extraction of each sample was pipetted into a 96-well plate and the absorbance was measured by a microplate reader (Spark, TECAN) under 540 nm. The absorbance was further normalized by DNA amount. Triplicate samples were used for the analysis to calculate means and standard deviations (n = 3).

Osteogenesis-related staining and quantification

Alkaline phosphatase (ALP), which is expressed in the early stage of osteogenic differentiation was stained after hMSCs were cultured in the osteogenic induction media for 7 d. Briefly, the staining working solution was prepared by dissolving naphthol AS-MX phosphate (N4875, Sigma-Aldrich) and fast blue RR salt (F0500, Sigma-Aldrich) in 56 mM 2-amino-2-methyl-1,3-propanediol (pH 9.9, A9754, Sigma-Aldrich) to reach a final concentration of 0.1%. The cells were rinsed with PBS twice and then fixed with 4% paraformaldehyde for 5 min at 4 ℃. The fixed cells were soaked in the above-mentioned staining working solution for 10 min at room temperature in the dark. Finally, PBS was used to cover the cells and the staining was checked under an optical microscope (BZ-X710).

After 21 d of osteogenic induction culture, calcium nodules were visualized and quantified by Alizarin Red staining. Alizarin Red S (400480250, Acros Organics) was weighed and dissolved in Milli-Q water to reach a concentration of 0.5%. The pH was adjusted to 4.2 before use. After the cells were fixed by 4% paraformaldehyde for 10 min at 4 ℃ and processed by two Milli-Q water washings, the cells were soaked in 300 μl of 0.5% alizarin red for 2 min at room temperature. Finally, the samples were washed with Milli-Q water again and their phase-contrast photos were recorded by BZ-X710. For quantification, the samples were dried in the air and then 350 μl of diluted 5% perchloric acid (166-0073, Wako) was added into each well. After incubating for 20 min at room temperature, 100 μl of the lysates were transferred to a 96-well plate. The absorbance of each well was recorded under 405 nm by using a Spark microplate reader. The absorbance was further normalized by DNA amount. Triplicate samples were used to calculate means and standard deviations (n = 3).

RNA isolation and gene expression analysis

After the cells were cultured in differentiation induction media for 21 d, the media were removed and cells were washed with warmed PBS twice. Thereafter, 1 ml of Sepasol RNA I Super G (09379-97, nacalai tesque) was added into each well to extract RNA. Based on the instructions, chloroform was added to extract RNA through phase separation. After 2-propanol precipitation and 75% ethanol washing, the extracted RNA was redissolved in nuclease-free water (Thermo Fisher Scientific, USA). The concentration of the extracted RNA was measured with a NanoDrop^{TM} Lite Spectrophotometer (Thermo Fisher Scientific, USA) and unified with nuclease-free water to get the same concentration for different samples. cDNA library was built by employing a High-Capacity cDNA Reverse Transcription Kit (4374966, Applied Biosystems). A 7500 Real-Time PCR system (Applied Biosystem, USA) was used to perform real-time PCR. The expression level of GAPDH which is a housekeeping gene was used as an endogenous control and the target gene expression relative to GAPDH was calculated with a $2^{-\triangle\triangle Ct}$ method. The normal viscosity group (without PEG supplement) was used as a reference. GAPDH (Hs99999905_m1, lot: 2104444, applied biosystems), CEBPA (Hs00269972_s1, lot: 1993980, applied biosystems), FASN (Hs00188012_m1, lot: 1875477, applied biosystems), FABP4 (Hs00609791_m1, lot: 1909263, applied biosystems) and LPL (Hs00173425_m1, lot: 1953315, applied biosystems) were used for the adipogenic differentiation. For osteogenic differentiation, ALPL (Hs01029144_m1, lot: 2103375, applied biosystems), BMP2 (Hs00154192_m1, lot: 2090101, applied biosystems), RUNX2 (Hs00231692_m1, lot: 2080647, applied biosystems) and SPP1 (Hs00959010_m1, lot: 2095770, applied biosystems) were used. Triplicate samples were used for the analysis to calculate means and standard deviations (n = 3).

Immunofluorescence staining of differentiation and mechanotransduction-related proteins

FABP4 and osteopontin (OPN) immunofluorescence staining were performed for adipogenic and osteogenic differentiation, respectively. To examine the underlying mechanism, two mechanotransduction proteins (YAP and β-catenin) were immunofluorescently stained in each differentiation process. For the staining of differentiation markers (FABP4 and OPN), 50,000 cells were seeded into each well of a 24-well plate, while for the visualization of mechanotransduction-related proteins, 320 µl of cell suspensions at the concentration of 18,000 cells/ml were added into each well of a 48-well plate. After culture for 24 h post seeding, the media were changed to the differentiation induction media. After the cells were cultured in the induction medium for 3 d (for differentiation markers) or 24 h (for mechanotransduction markers), the media were removed and the cells were fixed with 4% paraformaldehyde for 15 min at room temperature. The cells were stained according to the standard immunofluorescence procedures. Briefly, after the cells were blocked in a blocking buffer (1X PBS/5% normal serum/0.3% Triton X-100) for 60 min at room temperature, they were incubated with anti-FABP4 (rabbit-derived, 1:200 dilution, ab92501, abcam), anti-osteopontin (rabbit-derived, 1:200 dilution, ab63856, abcam), anti-YAP (mouse-derived, 1:50 dilution, sc-101199, Santa Cruz) or anti-β-catenin (rabbit-derived, 1:200 dilution, 8480, Cell Signaling

Technology) overnight at 4 ℃ followed by washing with PBS thrice, respectively. The antibodies were diluted by antibody dilution buffer (1X PBS/1% BSA/0.3% Triton X-100). Thereafter, cells were incubated in secondary antibodies for 2 h at room temperature in the dark. For the YAP antibody, Alexa Fluor 488 donkey anti-mouse lgG (1:500 dilution, H+L, A21202, Invitrogen) was used. For the other antibodies, Alexa fluor 488 goat anti-rabbit lgG (1:500 dilution, H+L, A11008, Invitrogen) was used. In addition, cell nuclei were stained with Hoechst 33258 (1:1000 dilution, 343-07961, FUJIFILM Wako Pure Chemical) for 10 min at room temperature. Finally, the stained cells were observed and recorded through a fluorescence microscope (BZ-X710). Image analysis was performed in CellProfiler (Broad Institute). The YAP and β-catenin nuclear/cytoplastic ratios were determined by dividing the average fluorescence intensity in the nucleus by the average fluorescence intensity in the cytoplasm. Over 30 cells were taken into the analysis.

Western blot analysis of mechanotransduction-related proteins

For the western blot analysis of mechanical-related proteins, the cells were seeded into each well of a 6-well plate (2.5 ml, 9.6×10^4 cells/ml). After exposure to different viscous stimuli for 3 d in adipogenic and osteogenic induction media, the cells were lysed in 200 μl RIPA buffer (sc-24948, Santa Cruz) containing PMSF, sodium orthovanadate and protease inhibitor cocktail. Then, the protein concentrations were measured and normalized by a Pierce BCA Protein Assay Kit (23225, Thermo Scientific). The samples were mixed with 4X Laemmli sample loading buffer (1610747, Bio-Rad) with 2-mercaptoethanol addition. Thereafter, proteins were separated in 10% denaturing acrylamide gels and subsequently transferred to a PVDF membrane (0.2 μm, 162-0175, Bio-Rad) by a semi-dry transmembrane method. The membrane was blocked in blocking buffer (5% BSA in 1X TBST) for 1 h at room temperature after washing with TBS buffer. Then, the membrane was washed by TBST thrice and probed with primary antibodies overnight at 4 ℃. The primary antibodies included YAP (14074, Cell Signaling), β-catenin (8480, Cell Signaling) and GAPDH (14C10, Cell Signaling) which served as an internal reference. After primary antibody incubation, the HRP-conjugated secondary antibody (K4003, Dako) was employed and the membrane was incubated for 1 h at room temperature with gentle agitation. Finally, the immune-reactive bands were visualized with the DAB method (K3468, Dako). The band image was acquired by an Amersham Typhoon (Cytiva).

Statistical analysis

The data were presented as means ± standard deviation (SD). For Oil Red O absorbance, Alizarin Red absorbance, gene expression, osmolarity measurement, as well as immunofluorescence staining data, a one-way analysis of variance (ANOVA) with Tukey's post hoc test for multiple comparisons was employed. For DNA quantification, a two-way ANOVA was used instead. Statistical analyses were processed by Prism GraphPad (version 10.1.2, USA). Significance levels were set at $*p < 0.05$, $**p < 0.01$, $***p < 0.001$ and $****p < 0.0001$.

Results

Viscosity of culture medium

The viscosity of the cell culture medium was modulated by supplementing PEG with different molecular weights. The final concentration of PEG in the viscous media was 1.0% (w/v%). Normal culture medium without PEG supplementation was served as a control. The viscosity of the media decreased with the increase of shear rate (Figure 1a and 1b). The two types of differentiation induction media (adipogenic and osteogenic induction media) showed a similar viscosity rheological profile. The zero-shear viscosity of the high viscosity group (denoted as H-V) was 645.5 ± 74.7 cP for adipogenic medium and 650.8 ± 60.6 cP for osteogenic medium. That of the middle viscosity group (denoted as M-V) was 268.9 ± 46.6 cP for adipogenic medium and 244.6 ± 47.8 cP for osteogenic medium. The low viscosity group (denoted L-V) had viscosity of 88.8 ± 32.1 cP for adipogenic medium and 105.9 ± 23.8 cP for osteogenic medium. The viscosity of medium without PEG supplementation (denoted as N-V) was 74.2 ± 23.6 cP for adipogenic medium and 86.4 ± 28.2 cP for osteogenic medium. Therefore, the viscosity range of the adipogenic and osteogenic induction media could be modulated from 74.2 to 650.8 cP by adjusting the molecular weight of PEG while keeping the PEG concentration at the same level. The detailed composition and viscosity of each viscous induction solution were listed in Table S1. The viscosity range in this study was larger than the previous studies [19–21]. Furthermore, osmolarity of the viscous media may also affect cell behaviour and cell differentiation fate [22]. Thus, we measured the osmolarity of both adipogenic and osteogenic medium (Figure S1). The osmolarity of all the adipogenic induction media was not significantly different. Similarly, the osmolarity of all the osteogenic induction media had no significant difference. The addition of 1.0 w/v% PEG in the culture media did not significantly affect the osmolarity of either adipogenic induction media or osteogenic induction media. Thus, the interference of osmolarity on cell viability and differentiation could be ignored in this study. The osmolarity of adipogenic media was higher than that of the osteogenic media due to the different supplements and concentrations in the two types of induction media. It has been reported that osmolarity value is dependent on the measurement techniques and the supplements [23–25]. It has also been reported that adipose-derived stem cells cultured in high osmolarity media up to 600 mOsm/L are alive with a high viability [26].

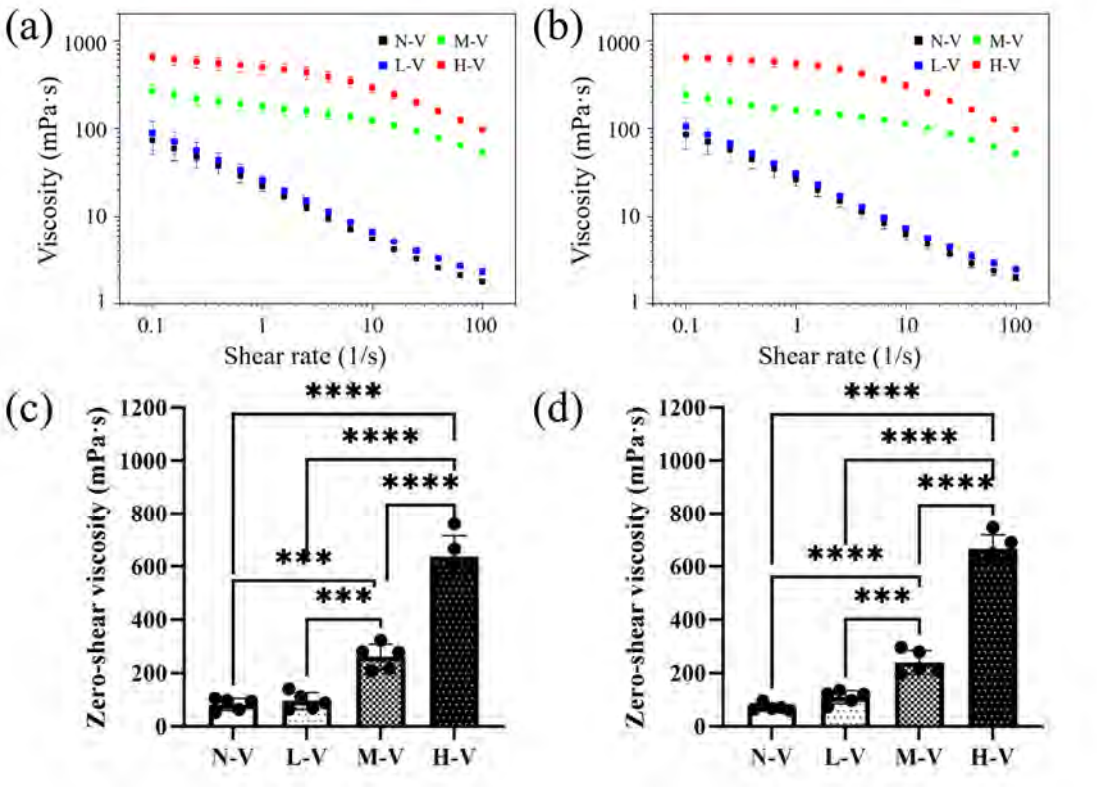

Figure 1. Viscosity against shear rate (a, b) and the corresponding zero-shear viscosity (c, d) of different culture medium. (a, c) Adipogenic induction medium. (b, d) Osteogenic induction media. N-V represents the normal induction medium without PEG supplementation. L-V, M-V and H-V represent the PEG-supplemented induction medium of low viscosity, middle viscosity and high viscosity, respectively. Data are shown as mean ± SD (n = 5). Significant difference: *** $p < 0.001$, **** $p < 0.0001$.

Cell viability, proliferation and morphology

Fibronectin was coated on the 24-well plates before cell culture. Strong green fluorescence of the immunological staining photomicrograph indicated the presence of coated fibronectin on the wells of 24-well plates (Figure S2). After hMSCs were seeded in the fibronectin-coated 24-well plates and pre-cultured for 24 h, the culture medium was changed to the corresponding normal, low, middle and high-viscosity induction media. Before the medium was changed to the viscous media, live/dead staining was performed to check cells' initial viability. As shown in Figure 2a, almost all the cells were alive before viscosity stimulus treatment. Thereafter, the cells were continuously cultured in the viscous induction media. After 21 d of culture, almost all the cells under different induction were alive with only a few dead detected (Figure 2b and 2c). The cell density after culturing in the adipogenic induction media for 21 d became a little denser, while cells cultured in the osteogenic induction media became much denser than the cells before the medium changed to induction media.

The amount of DNA in each group was quantitatively evaluated to investigate the effect of viscosity on hMSCs proliferation during adipogenic and osteogenic differentiation. DNA amount was almost the same, around 0.6 μg/well before the medium was changed to the viscous induction media (Figure 2d and 2e). It was because the same number of cells were seeded in each well. When the cells were cultured in adipogenic induction media, the increase in DNA amount was very small. In contrast, the cells cultured in the osteogenic induction media increased with culture time (Figure 2e). The different proliferation behaviours in adipogenic and osteogenic induction media should be owing to the changes of cell cytoskeleton architectures during adipogenesis and osteogenesis (Figure S3 and S4). During adipogenesis, actin filaments were partially disassembled with the ongoing of induction, resulting in a relatively rounded cell morphology and a disrupted actin network. The actin filaments were assembled and predominantly distributed along the peripheral regions of the cells. On the other hand, during osteogenic differentiation, actin filaments were assembled both at the peripheral regions and across the cells. The cells during the adipogenic and osteogenic differentiation showed the same cytoskeleton re-organisation as the previous reports [27–29]. Thus, cell proliferation was hindered in adipogenic induction media, while promoted in osteogenic induction media. Cell proliferation in high viscosity medium was lower than that in low viscosity medium. High viscosity had a negative effect towards cell proliferation. Furthermore, we also did the apoptosis assay to evaluate cell apoptosis in different groups. As shown in Figure S5, cell apoptosis was not obviously observed in any of the different viscous groups. The results suggested that viscosity did not induce cell apoptosis.

Moreover, the cells were monitored during adipogenic and osteogenic induction culture by following the phase-contrast photos of cells on 0, 7, 14 and 21 d of induction culture (Figure S6 and S7). During adipogenesis, lipid vacuoles were formed and became more evident with the extension of induction time. Apparently, more lipids were formed in low viscosity groups compared to the middle and high viscosity groups (Figure S6), indicating that high viscosity was detrimental to adipogenesis. Intriguingly, for osteogenesis, nodule-like structures were deposited more in the middle and high viscosity groups than the normal and low viscosity groups (Figure S7), reflecting the beneficial effects of high viscosity towards osteogenesis.

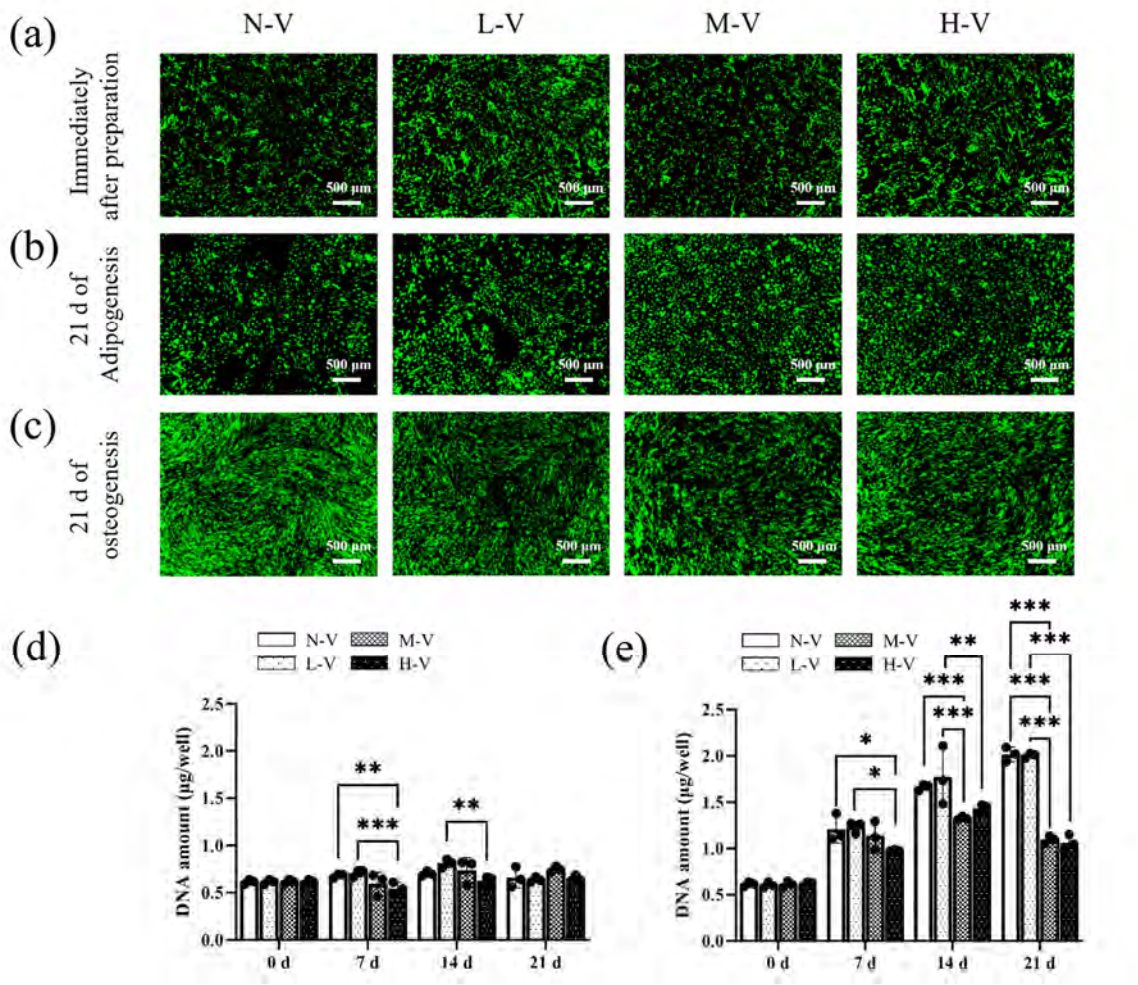

Figure 2. Live/dead staining (a-c) and DNA quantification (d, e) of hMSCs cultured in induction medium of different viscosity. Cells were stained before (a) and after (b, c) culture in adipogenic and osteogenic induction media of different viscosity for 21 d. Scale bar = 500 μm. DNA amount was measured after culture in adipogenic (d) and osteogenic (e) induction media for 0, 7, 14 and 21 d. Data represent mean ± SD (n = 3). Significant difference: $*p < 0.05$, $**p < 0.01$, $***p < 0.001$.

Influence of viscosity on adipogenic differentiation

After culturing in adipogenic induction media of different viscosity for 3 d, 14 d and 21 d, the influence of viscosity on adipogenic differentiation of hMSCs was investigated by FABP4 immunofluorescence staining, Oil Red O staining and expression analysis of adipogenesis-related genes, respectively. As shown in the stained cells (Figure 3a), the adipogenic-related marker FABP4 was expressed more in low viscosity groups. More oil droplets were accumulated in the normal and low viscosity groups compared to the middle and high viscosity groups (Figure 3b). Quantification of the stained oil droplets further

demonstrated that the adipogenic degree decreased with the increase of solution viscosity (Figure 3c). Furthermore, four adipogenic-related gene expressions were checked: CCAAT/enhancer binding protein (CEBPA), fatty acid synthase (FASN), fatty acid binding protein 4 (FABP4) and lipoprotein lipase (LPL) (Figure 3d-3g). The relative expression of these genes was decreased with the increase of solution viscosity. Thus, the results indicated that low viscosity was beneficial for adipogenic differentiation.

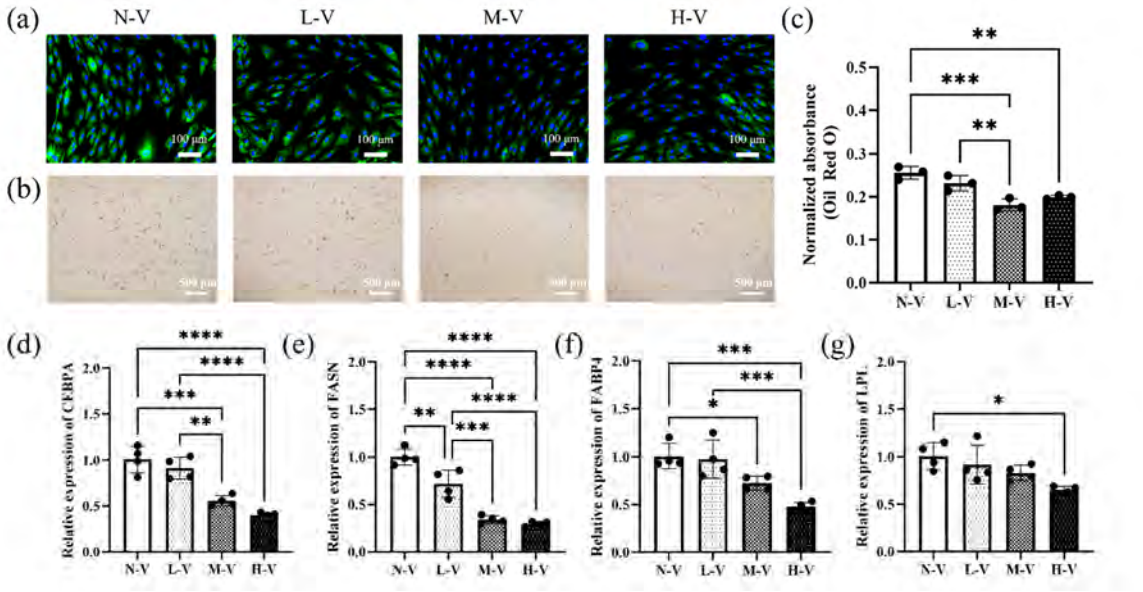

Figure 3. Influence of viscosity on adipogenic differentiation of hMSCs cultured in adipogenic induction medium of different viscosity. Immunofluorescence staining of FABP4 expressed in hMSCs after culturing in viscous adipogenic induction medium for 3 d, scale bar = 100 μm, green fluorescence indicates FABP4 and blue fluorescence indicates cell nuclei (a). Oil Red O staining after culturing for 14 d (b), scale bar = 500 μm. Absorbance at 540 nm of the Oil Red O dye extracted from the stained cells (c), n = 3. Gene expression (n = 4) of CEBPA (d), FASN (e), FABP4 (f) and LPL (g) of hMSCs cultured in adipogenic induction medium of different viscosity for 21 d. Data were normalized by the respective gene expression level of hMSCs cultured in the normal induction medium without PEG supplement. Data represent mean ± SD. Significant difference: *$p < 0.05$, **$p < 0.01$, ***$p < 0.001$, **** $p < 0.0001$.

Influence of viscosity on osteogenic differentiation

For osteogenesis, after hMSCs were cultured in osteogenic induction media of different viscosity for 3 d, the osteogenic-related marker OPN was stained (Figure 4a). The fluorescence intensity was higher in the high viscosity counterparts (Figure 4a). Besides, the staining of ALP which is a marker of early osteogenesis was also performed (Figure 4b). ALP staining in the middle and high viscosity groups was stronger than that in the normal and low viscosity groups. Furthermore, after the cells were cultured for 21 d,

alizarin red staining was performed to reflect calcium deposition (Figure 4c). The results showed that more calcium deposition was observed in the cells cultured in the high viscosity groups than those in low viscosity groups. Quantification of the stained Alizarin Red showed the amount of calcium deposition significantly increased with the viscosity of the induction media (Figure 4d). Expression of four major osteogenic-related genes such as alkaline phosphatase (ALPL), bone morphogenetic protein 2 (BMP2), runt-related transcription factor-2 (RUNX2) and secreted phosphoprotein 1 (SPP1) was analyzed (Figure 4e-4h). Expression of all these osteogenic-related genes increased with the increase of viscosity. Thus, high viscosity could facilitate osteogenic differentiation of hMSCs.

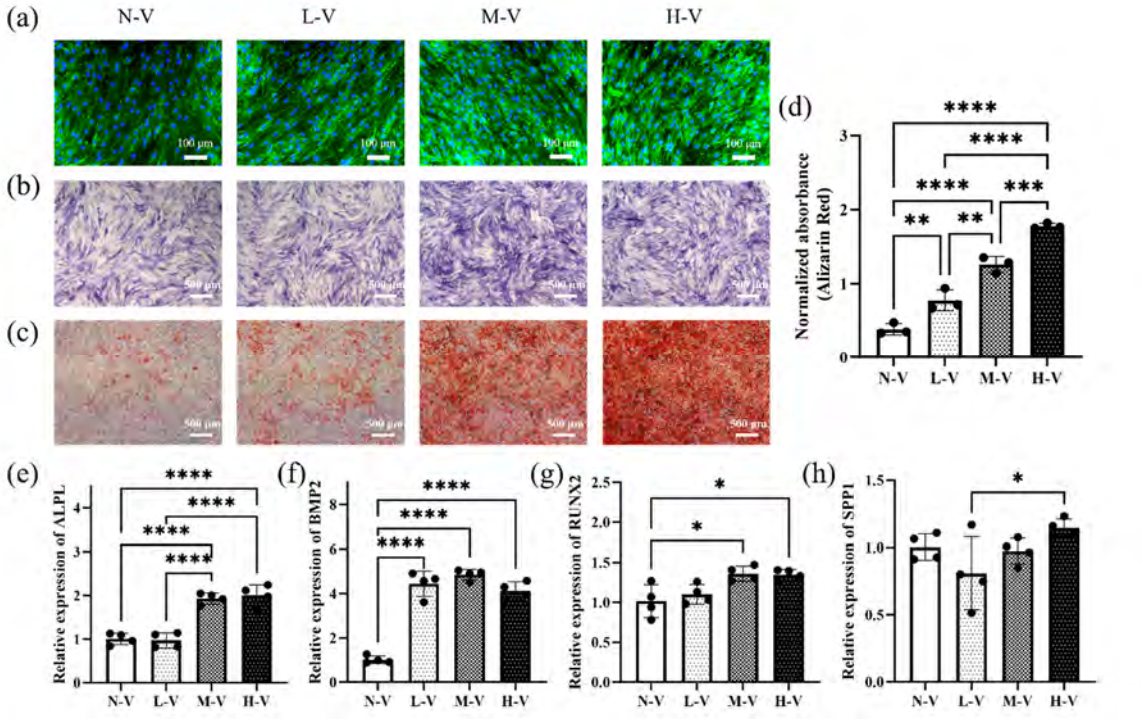

Figure 4. Influence of viscosity on osteogenic differentiation of hMSCs cultured in osteogenic induction medium of different viscosity. Immunofluorescence staining of OPN expressed in hMSCs after culturing in viscous osteogenic induction medium for 3 d, scale bar = 100 μm, green fluorescence indicates OPN and blue fluorescence indicates cell nuclei. ALP staining after cultured for 7 d (b) and Alizarin Red staining after cultured for 21 d (c), scale bar = 500 μm. Absorbance at 405 nm of the Alizarin Red extracted from the stained cells (d), n = 3. Gene expression (n = 4) of ALPL (e), BMP2 (f), RUNX2 (g) and SPP1 (h) of hMSCs cultured in adipogenic induction medium of different viscosity for 21 d. Data were normalized by the respective gene expression level of hMSCs cultured in the normal induction medium without PEG supplement. Data represent mean ± SD. Significant difference: *$p < 0.05$, **$p < 0.01$, ***$p < 0.001$, **** $p < 0.0001$.

Influence of viscosity on mechanotransduction-related proteins

As revealed by many studies, mechanotransduction plays a pivotal role in deciding cell functions and differentiation fates of stem cells [1,30]. The process is initiated by mechanosensation, which involves cell-cell interaction, cell-matrix interaction, as well as environmental stimulating factors such as viscosity and shear stress. Among these pathways, yes-associated protein (YAP)/transcriptional coactivator with PDZ-binding motif (TAZ) are primary sensors of the cell's physical nature [31] and they have also been shown to act as mechanical sensors [32,33]. The phosphorylation and dephosphorylation of YAP/TAZ are related to adipogenic and osteogenic fates of stem cells [32,33]. Additionally, Wnt/β-catenin signalling is another pathway involved in osteogenic commitment [2,34]. Under activation of β-catenin pathways, hypophosphorylated β-catenin can translocate into the cell nucleus, where it interacts with transcription factors of the T-cell factor/lymphocyte enhancer factor, further inducing RUNX2 transcription to facilitate osteogenesis [35–37]. Thus, both YAP and β-catenin were immunostained to explore the underlying mechanisms of the influence of viscosity towards hMSCs adipogenic and osteogenic differentiation. As shown in Figure 5a, during adipogenesis, YAP was primarily localized in the cell nucleus with the increase of viscosity. The ratio of nuclear YAP/cytoplastic YAP significantly increased with the viscosity of culture media (Figure 5c). However, β-catenin was predominantly presented on the cell membrane and cytoplasm (Figure 5b). There was no statistical difference among the normal, low, middle and high viscosity groups. The results were further verified by western blot, where YAP was sustained more in the high viscosity groups. However, the change of β-catenin bands was not evident (Figure 5e).

During osteogenic differentiation, YAP nuclear localization showed a similar pattern to that of adipogenesis and the ratio of nuclear YAP/cytoplasmic YAP showed a significant increase with viscosity (Figure 6a and 6c). The nuclear β-catenin localization showed a more apparent tendency with the increase of viscosity and the ratio of nuclear β-catenin/cytoplasmic β-catenin significantly increased with the viscosity of culture medium (Figure 6c and 6d). Western blot analysis of YAP and β-catenin expression also showed a similar change profile, where these proteins were sustained more in the high viscosity groups (Figure 6e).

The results indicated that the nuclear localization of both YAP and β-catenin increased with the increase of viscosity during osteogenic differentiation. A high degree of YAP and β-catenin nuclear localization has been reported responsible for increased osteogenesis [32,38]. During adipogenic differentiation, the nuclear localization of YAP increased with the increase of viscosity, while β-catenin did not show obvious change. Nuclear localization of YAP has been reported to decrease adipogenesis [39].

Based on these results, high viscosity could facilitate nuclear localization of YAP and β-catenin and thus enhance osteogenesis, while high viscosity promoted nuclear localization of YAP, attenuating adipogenesis.

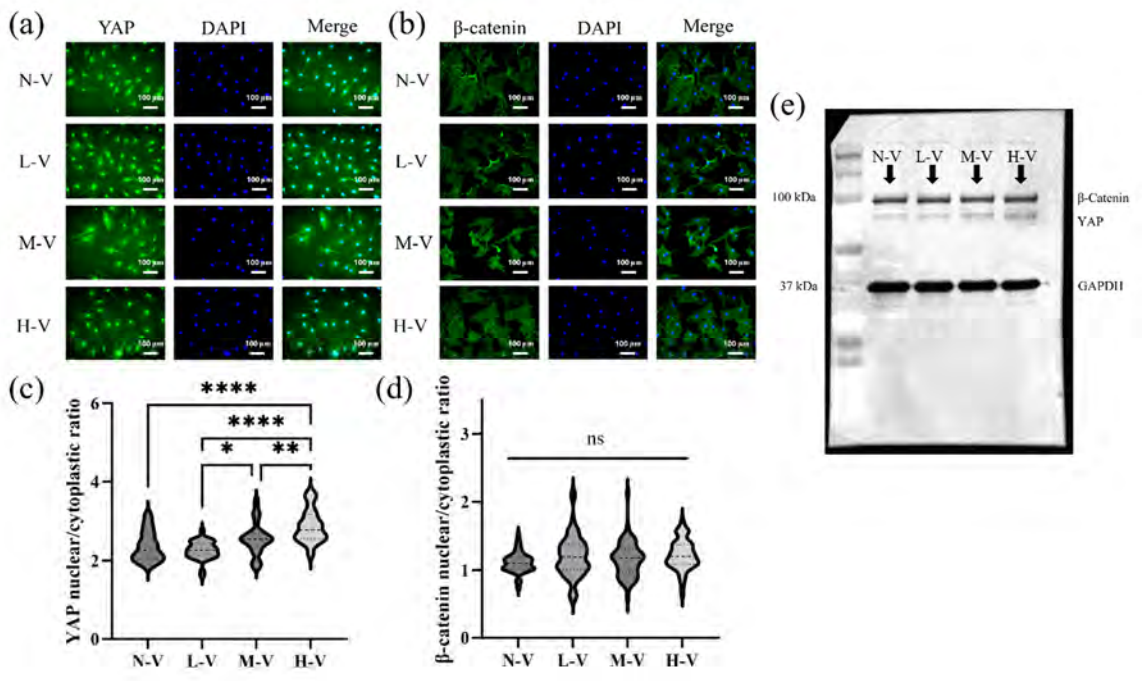

Figure 5. Influence of viscosity on nuclear translocation of mechanotransduction regulators (YAP and β-catenin) of hMSCs during adipogenic differentiation in the medium of different viscosity. Representative immunofluorescence staining of YAP (a) and β-catenin (b) after culture for 24 h. Cell nuclei were also stained (blue), scale bar = 100 μm. Quantification of the ratio of fluorescence intensity of nuclear YAP/cytoplastic YAP (c) and nuclear β-catenin/cytoplastic β-catenin (d), n > 30. Western blotting of YAP and β-catenin (e). Data represent mean ± SD. Significant difference: *$p < 0.05$, **$p < 0.01$, ***$p < 0.001$, **** $p < 0.0001$.

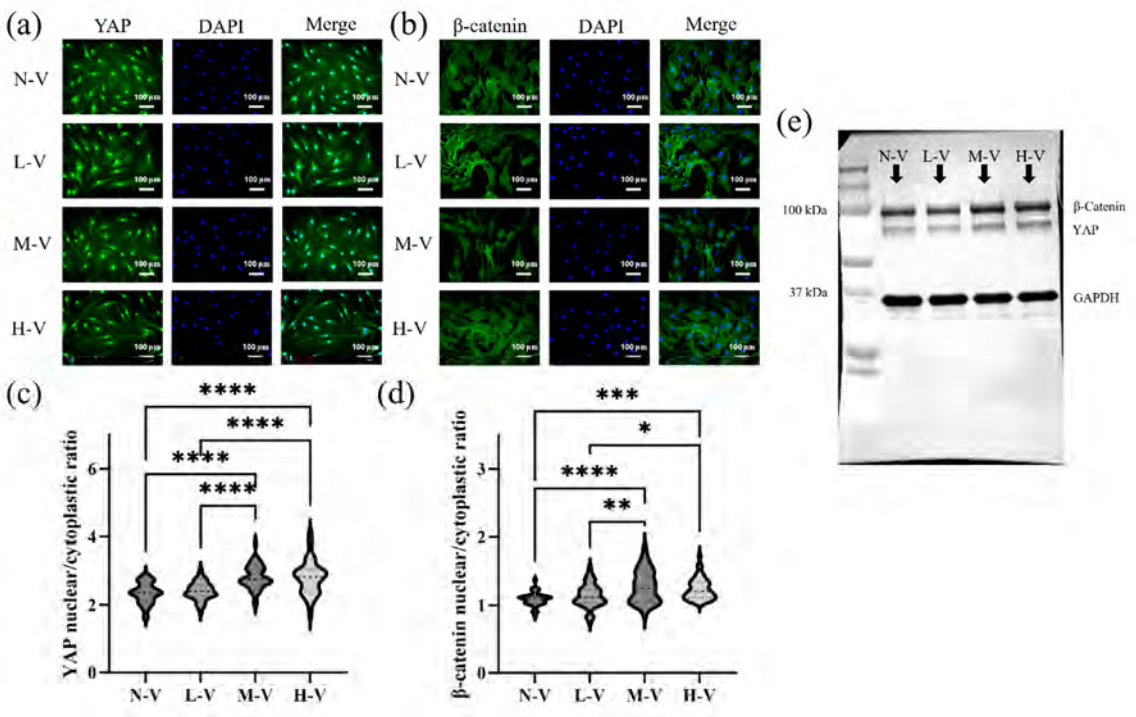

Figure 6. Influence of viscosity on nuclear translocation of mechanotransduction regulators (YAP and β-catenin) of hMSCs during osteogenic differentiation in the medium of different viscosity. Representative immunofluorescence staining of YAP (a) and β-catenin (b) after culture for 24 h. Cell nuclei were also stained (blue), scale bar = 100 μm. Quantification of the ratio of fluorescence intensity of nuclear YAP/cytoplastic YAP (c) and nuclear β-catenin/cytoplastic β-catenin (d), n > 30. Western blotting of YAP and β-catenin (e). Data represent mean ± SD. Significant difference: *$p < 0.05$, **$p < 0.01$, ***$p < 0.001$, **** $p < 0.0001$.

Discussion

Numerous efforts have been attributed to unravelling the influence of physical cues on cell functions. However, as an important part of physical cues, viscosity study remains in its infancy [5,40]. Therefore, in this study, we explored how viscosity affects hMSCs differentiation on a 2D substrate. PEG was chosen for its bioinert property and its convenience for viscosity adjustment [16,17,41]. The viscosity achieved ranged from 70.2~650.8 cP, which was wider than those used in previous studies and could reveal cell behaviours in a viscosity range approaching to the physiological conditions [8,9,13]. Meanwhile, the osmolarity difference in the culture media before and after PEG addition could be ignored (Figure S1), since the molar concentration of PEG in each medium was relatively low. The viscosity range in this study could partially reflect the viscous characteristics of synovial fluid and bone marrow. The results may provide some useful

information to predict how the viscous microenvironments in synovial fluid and bone marrow affect the osteogenesis and adipogenesis of stem cells.

In this paper, we used 2D culture, which differentiates from the 3D culture in terms of the degree of cell-cell and cell-matrix interaction perceived by cells. When cells are cultured in 3D viscous condition by using plasma-treated μPCL (poly-ε-caprolactone microparticles), RGD-conjugated microgels and GelMA hydrogels, the cells can interact with these matrices, therefore attaching to the matrices [15,21]. Cells can spread and proliferate normally in these matrices and higher viscosity facilitates osteogenesis [15,21]. Intriguingly, when cells are suspended in viscous culture medium without attaching to the matrices, cells form spheroids spontaneously and viscosity shows an inhibitory effect on differentiation [12], which reveals the importance of balance between cell-cell and cell-matrix interactions in perceiving external mechanical stimuli. In our study, the cells were cultured on cell culture plates in viscous medium, which was similar to the former 3D condition where the cells can attach on the matrices and the influence of viscosity on osteogenesis was also the same.

The proliferation of hMSCs was dependent on viscosity and cell phenotype. During adipogenesis, the cell population was almost kept constant. This might be attributed to the perturbed actin filaments during adipogenesis because their assembly and disassembly are important during cell proliferation [27]. Thus, cell proliferation was suspended during adipogenesis, which has also been proven by previous studies [42]. Viscosity did not show a significant influence on cell proliferation during adipogenesis. However, during osteogenesis, the cells proliferated with culture time and viscosity could suppress cell proliferation.

Besides the influence of viscosity on cell proliferation during osteogenesis, it also showed a significant influence on both adipogenesis and osteogenesis. High viscosity inhibited adipogenesis, as shown by the decreased oil droplet formation and decreased adipogenesis-related gene expression in high viscosity induction medium. High viscosity facilitated osteogenesis, as proven by elevated ALP activity, calcium deposition and osteogenic-related gene expressions. Some previous studies have reported that high stiffness and viscous dissipation could promote osteogenesis [7,43].

However, almost no reports have reported how a pure viscous system affects cell differentiation and proliferation. Except for one recently published paper explored by employing methylcellulose to modulate medium viscosity, showing that viscosity may activate TRPV4 (transient receptor potential vanilloid sub-type 4) and subsequently induce the translocation of YAP and regulate stem cell differentiation fate [44]. Mechanotransduction is a complex process involving many pathways and many external stimuli can activate these pathways, such as contractility, shear stress, biochemical stimuli, hypotonic or hypertonic stimuli, matrix viscoelasticity, etc. Most of the pathways converge to YAP/TAZ and β-catenin [45–47]. For instance, the activation of cadherin due to cell-cell interaction can induce actomyosin contractility and further activate YAP/TAZ and Lamin A/C [48]. The activation of TRPV4 or focal adhesions (induced by cell-matrix interaction) can subsequently activate RhoA pathway which is an upstream pathway of YAP/TAZ [17,49]. Furthermore, Wnt/β-catenin pathway is also a critical pathway involved in adipogenesis

and osteogenesis, which can be activated by mechanical stimuli and the downstream of the pathway also participates in TRP channels [49]. Thus, YAP/TAZ and β-catenin are the hubs during adipogenic and osteogenic differentiation. These signaling pathways do not interplay. Therefore, we explored these two key proteins related to mechanotransduction. By investigating YAP and β-catenin localization, we found that high viscosity could promote nuclear localization of both YAP and β-catenin during osteogenic differentiation. The high ratio of YAP and β-catenin in nucleus compared to the cytoplasm was responsible for the elevated osteogenesis [50]. Based on the results, we hypothesized that high viscosity facilitated YAP and β-catenin nuclear localization, thereby promoting osteogenesis-related gene expression and osteogenesis (Figure 7). During adipogenic differentiation, high viscosity promoted nuclear localization of YAP, but not β-catenin. The dominant pathway might be through the YAP signal pathway, not the Wnt/β-catenin signal pathway (Figure 7). Based on the results, we hypothesized that high viscosity facilitated YAP and β-catenin nuclear localization, thereby promoting osteogenesis. YAP might be the dominant signal pathway for the inhibitory effect of high viscosity on adipogenesis.

As indicated by the results, viscosity plays a pivotal role in the realm of stem cell differentiation. By changing the viscosity of cell culture media, we could guide the cell differentiation fate. Elucidation of viscosity influence on the proliferation and differentiation of stem cells can not only help to understand the interaction between stem cells and their viscoelastic microenvironments but also provide useful information for the design of cell culture systems and scaffolds for tissue engineering applications. Cell culture systems and scaffolds mimicking the viscous characteristics of the cellular microenvironment should be considered for the commitment of stem cells and functional tissue engineering. Overall, we believe the viscosity study could benefit the area of tissue engineering.

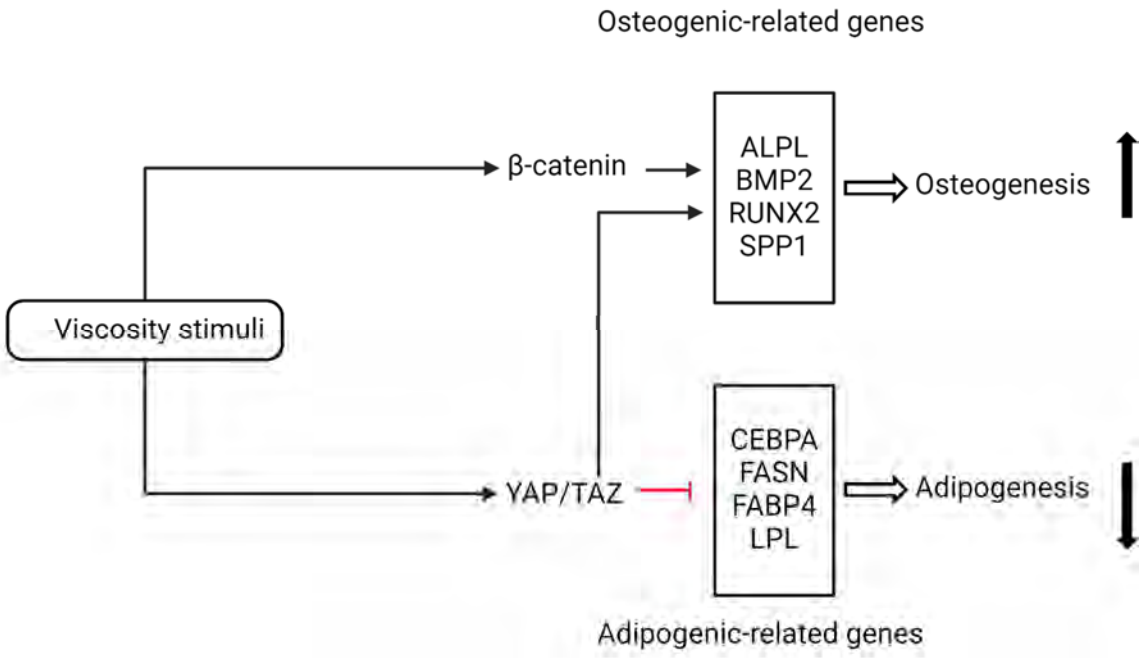

Figure 7. Models of how viscosity modulates adipogenesis and osteogenesis through β-catenin and YAP pathways.

Conclusions

The influence of viscosity on adipogenic and osteogenic differentiation of hMSCs was revealed in this study in a 2D manner. High viscosity could promote osteogenesis while inhibiting adipogenesis. The elevated osteogenesis was related to both the increased YAP and β-catenin nuclear translocation, while the decreased adipogenesis was related to the increased YAP nuclear translocation. The results revealed the importance of viscosity in determining the hMSCs differentiation fates.

Acknowledgements

We thank Dr. Atsushi Matsuoka, Research Center for Membrane and Film Technology, Kobe University, for the measurement of osmolarity. This research was supported by JSPS KAKENHI Grant Number 21H03830, 22K19926 and 24K03289.

References

1 Y. Zhang and P. Habibovic, *Advanced Materials*, 2022, **34**, 2110267.
2 Y. Shou, X. Y. Teo, K. Z. Wu, B. Bai, A. R. K. Kumar, J. Low, Z. Le and A. Tay, *Adv Sci (Weinh)*, 2023, e2300670.
3 X. Wang, X. Hu, J. Li, A. C. M. Russe, N. Kawazoe, Y. Yang and G. Chen, *Biomater. Sci.*, 2016, **4**, 970–978.
4 A. Higuchi, Q.-D. Ling, Y. Chang, S.-T. Hsu and A. Umezawa, *Chem Rev*, 2013, **113**, 3297–3328.
5 B. Yi, Q. Xu and W. Liu, *Bioactive Materials*, 2022, **15**, 82–102.
6 T. Akasaka, M. Tamai, Y. Yoshimura, N. Ushijima, S. Numamoto, A. Yokoyama, H. Miyaji, R. Takata, S. Yamagata, Y. Sato, K. Nakanishi and Y. Yoshida, *Nano Res.*, 2022, **15**, 4201–4211.
7 C. Liu, Q. Yu, Z. Yuan, Q. Guo, X. Liao, F. Han, T. Feng, G. Liu, R. Zhao, Z. Zhu, H. Mao, C. Zhu and B. Li, *Bioactive Materials*, 2023, **25**, 445–459.
8 U. A. Gurkan and O. Akkus, *Ann Biomed Eng*, 2008, **36**, 1978–1991.
9 H. Fam, J. T. Bryant and M. Kontopoulou, *Biorheology*, 2007, **44**, 59–74.
10 W. Yao, Z. Shen and G. Ding, *Int J Biol Sci*, 2013, **9**, 1050–1056.
11 S. K. Lai, Y.-Y. Wang and J. Hanes, *Adv Drug Deliv Rev*, 2009, **61**, 158–171.
12 J. Zheng, H. Chen, C. Lu, T. Yoshitomi, N. Kawazoe, Y. Yang and G. Chen, *J. Mater. Chem. B*, 2023, **11**, 7424–7434.
13 J. Schurz and V. Ribitsch, *Biorheology*, 1987, **24**, 385–399.
14 K. Comley and N. A. Fleck, *International Journal of Solids and Structures*, 2010, **47**, 2982–2990.

15 M. Ghasemzadeh-Hasankolaei, J. M. Miranda, C. R. Correia and J. F. Mano, *Small Methods*, 2023, **7**, 2201503.
16 M. Pittman, E. Iu, K. Li, J. Chen, S. Potnikov and Y. Chen, *Biophys. J.*, 2022, **121**, 267A-267A.
17 K. Bera, A. Kiepas, I. Godet, Y. Li, P. Mehta, B. Ifemembi, C. D. Paul, A. Sen, S. A. Serra, K. Stoletov, J. Tao, G. Shatkin, S. J. Lee, Y. Zhang, A. Boen, P. Mistriotis, D. M. Gilkes, J. D. Lewis, C.-M. Fan, A. P. Feinberg, M. A. Valverde, S. X. Sun and K. Konstantopoulos, *Nature*, 2022, **611**, 365–373.
18 J. Zheng, Y. Wang, N. Kawazoe, Y. Yang and G. Chen, *J. Mater. Chem. B*, 2022, **10**, 3989–4001.
19 K. Lee, Y. Chen, X. Li, N. Kawazoe, Y. Yang and G. Chen, *Journal of Materials Science & Technology*, 2021, **63**, 1–8.
20 K. Lee, Y. Chen, X. Li, Y. Wang, N. Kawazoe, Y. Yang and G. Chen, *J. Mater. Chem. B*, 2019, **7**, 7713–7722.
21 K. Lee, Y. Chen, T. Yoshitomi, N. Kawazoe, Y. Yang and G. Chen, *Adv. Healthcare Mater.*, 2020, **9**, 2000617.
22 J. S.-H. Chui, T. Izuel-Idoype, A. Qualizza, R. P. de Almeida, L. Piessens, B. K. van der Veer, G. Vanmarcke, A. Malesa, P. Athanasouli, R. Boon, J. Vriens, L. van Grunsven, K. P. Koh, C. M. Verfaillie and F. Lluis, *Advanced Science*, 2024, **11**, 2307554.
23 M. J. Madden, S. N. Ellis, A. Riabtseva, A. D. Wilson, M. F. Cunningham and P. G. Jessop, *Desalination*, 2022, **539**, 115946.
24 D. N. Runckel and J. R. Swanson, *Clinical Chemistry*, 1980, **26**, 1745–1747.
25 K. Pollock, G. Yu, R. Moller-Trane, M. Koran, P. I. Dosa, D. H. McKenna and A. Hubel, *Tissue Eng Part C Methods*, 2016, **22**, 999–1008.
26 U. Potočar, S. Hudoklin, M. E. Kreft, J. Završnik, K. Božikov and M. Fröhlich, *PLOS ONE*, 2016, **11**, e0163870.
27 L. Blanchoin, R. Boujemaa-Paterski, C. Sykes and J. Plastino, *Physiological Reviews*, 2014, **94**, 235–263.
28 P. Mishra, R. Cohen, N. Zhao and P. Moghe, *Methods*, 2021, **190**, 44–54.
29 A. U. Khan, R. Qu, T. Fan, J. Ouyang and J. Dai, *Stem Cell Res Ther*, 2020, **11**, 283.
30 M.-K. Hayward, J. M. Muncie and V. M. Weaver, *Dev Cell*, 2021, **56**, 1833–1847.
31 S. Piccolo, S. Dupont and M. Cordenonsi, *Physiological Reviews*, 2014, **94**, 1287–1312.
32 J.-X. Pan, L. Xiong, K. Zhao, P. Zeng, B. Wang, F.-L. Tang, D. Sun, H.-H. Guo, X. Yang, S. Cui, W.-F. Xia, L. Mei and W.-C. Xiong, *Bone Res*, 2018, **6**, 18.
33 R. J. McMurray, M. J. Dalby and P. M. Tsimbouri, *J Tissue Eng Regen Med*, 2015, **9**, 528–539.
34 A. Mauviel, F. Nallet-Staub and X. Varelas, *Oncogene*, 2012, **31**, 1743–1756.
35 L. Yang, R. Dai, H. Wu, Z. Cai, N. Xie, X. Zhang, Y. Shen, Z. Gong, Y. Jia, F. Yu, Y. Zhao, P. Lin, C. Ye, Y. Hu, Y. Fu, Q. Xu, Z. Li and W. Kong, *Circ Res*, 2022, **130**, 213–229.
36 D. Fang, D. Hawke, Y. Zheng, Y. Xia, J. Meisenhelder, H. Nika, G. B. Mills, R. Kobayashi, T. Hunter and Z. Lu, *Journal of Biological Chemistry*, 2007, **282**, 11221–11229.

37 H. W. Park, Y. C. Kim, B. Yu, T. Moroishi, J.-S. Mo, S. W. Plouffe, Z. Meng, K. C. Lin, F.-X. Yu, C. M. Alexander, C.-Y. Wang and K.-L. Guan, *Cell*, 2015, **162**, 780–794.
38 L. Wang, X. You, L. Zhang, C. Zhang and W. Zou, *Bone Res*, 2022, **10**, 1–15.
39 J. Oliver-De La Cruz, G. Nardone, J. Vrbsky, A. Pompeiano, A. R. Perestrelo, F. Capradossi, K. Melajová, P. Filipensky and G. Forte, *Biomaterials*, 2019, **205**, 64–80.
40 W. Xie, X. Wei, H. Kang, H. Jiang, Z. Chu, Y. Lin, Y. Hou and Q. Wei, *Adv Sci (Weinh)*, 2023, **10**, e2204594.
41 H. Lu, L. Guo, N. Kawazoe, T. Tateishi and G. Chen, *J Biomater Sci Polym Ed*, 2009, **20**, 577–589.
42 M. P. Marquez, F. Alencastro, A. Madrigal, J. L. Jimenez, G. Blanco, A. Gureghian, L. Keagy, C. Lee, R. Liu, L. Tan, K. Deignan, B. Armstrong and Y. Zhao, *Stem Cells Dev*, 2017, **26**, 1578–1595.
43 Y. Wang, J. Zhang, X. Shu, F. Wu and J. He, *Chem. Eng. J.*, 2024, **482**, 149018.
44 Y.-Q. Chen, M.-C. Wu, M.-T. Wei, J.-C. Kuo, H. W. Yu and A. Chiou, *Materials Today Bio*, 2024, **26**, 101058.
45 X. Di, X. Gao, L. Peng, J. Ai, X. Jin, S. Qi, H. Li, K. Wang and D. Luo, *Sig Transduct Target Ther*, 2023, **8**, 1–32.
46 J. Hao, Y. Zhang, D. Jing, Y. Shen, G. Tang, S. Huang and Z. Zhao, *Acta Biomaterialia*, 2015, **20**, 1–9.
47 C. Loebel, R. L. Mauck and J. A. Burdick, *Nat. Mater.*, 2019, **18**, 883–891.
48 K. Wang, K. Man, J. Liu, B. Meckes and Y. Yang, *ACS Nano*, 2023, **17**, 2124–2133.
49 H. Shi, K. Zhou, M. Wang, N. Wang, Y. Song, W. Xiong, S. Guo, Z. Yi, Q. Wang and S. Yang, *Theranostics*, 2023, **13**, 3245–3275.
50 A. A. Bertrand, S. H. Malapati, D. T. Yamaguchi and J. C. Lee, *Advanced Healthcare Materials*, 2020, **9**, 2000709.

Supplementary Information

Table S1. Zero-shear viscosities of different viscous inductive media prepared by different ratios of PEG 35 K and PEG 8 M

Culture medium	PEG 35 K (w/v%)	PEG 8 M (w/v%)	Zero-shear viscosity of adipogenic medium (mPa·s)	Zero-shear viscosity of osteogenic medium (mPa·s)
Normal induction medium without PEG supplementation	0.00	0.00	74.2 ± 23.6	86.4 ± 28.2
Low viscosity	1.00	0.00	88.8 ± 32.1	105.9 ± 23.8
Middle viscosity	0.25	0.75	268.9 ± 46.6	244.6 ± 47.8
High viscosity	0.00	1.00	645.5 ± 74.7	650.8 ± 60.6

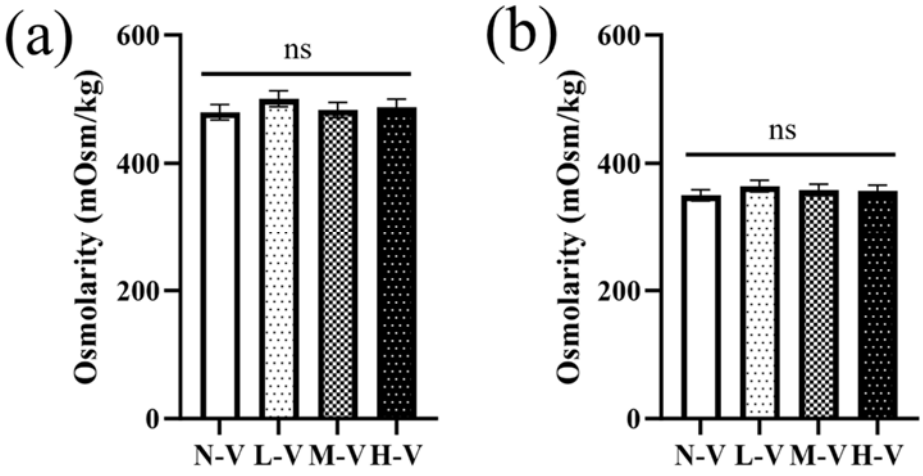

Figure S1. Osmolarity measurement of viscous induction media by the vapour pressure method. (a) Osmolarity measurement of different viscous adipogenic induction media. (b) Osmolarity measurement of different viscous osteogenic induction media. Data represent mean ± SD, n = 4. Significant difference: ns: not significant.

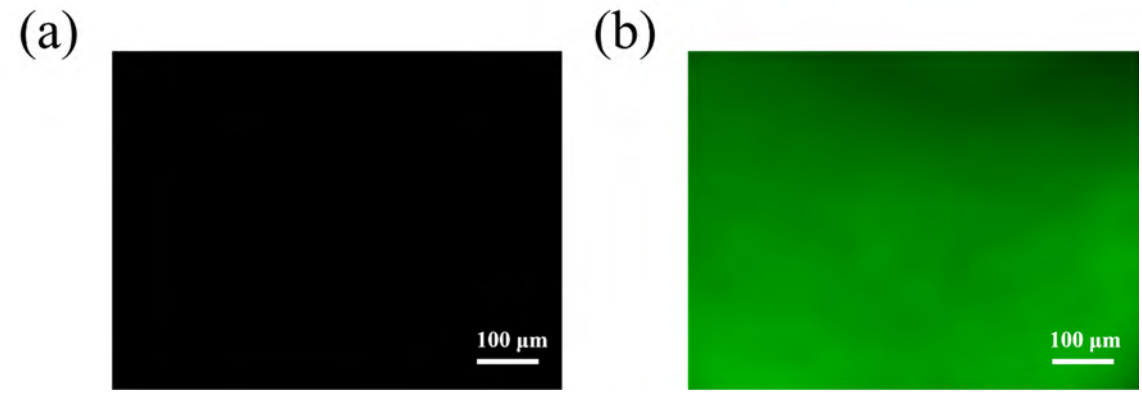

Figure S2. Characterization of fibronectin coating on a 24-well plate. (a) Without fibronectin coating. (b) With fibronectin coating. Scale bar = 100 µm.

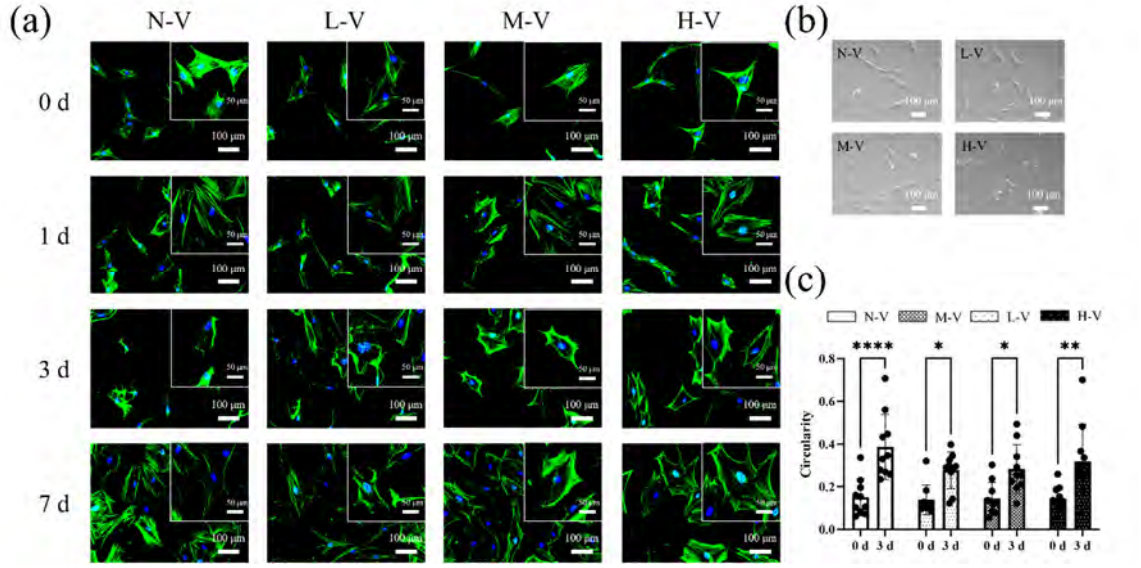

Figure S3. Morphology changes of hMSCs exposed to different viscous media under adipogenic differentiation. (a) F-actin staining of hMSCs under different viscosity exposure during adipogenic differentiation on 0, 1, 3 and 7 d. (b) Phase-contrast photomicrographs of hMSCs exposed to different viscous adipogenic induction media for 3 d. (c) Circularity change during adipogenic differentiation on 0 d and 3 d under different viscosities (circularity was calculated based on the equation: $Circularity = \frac{4\pi \times Area}{Perimeter^2}$). Data

represent mean ± SD. Significant difference: *$p < 0.05$, **$p < 0.01$, ***$p < 0.001$, ****$p < 0.0001$.

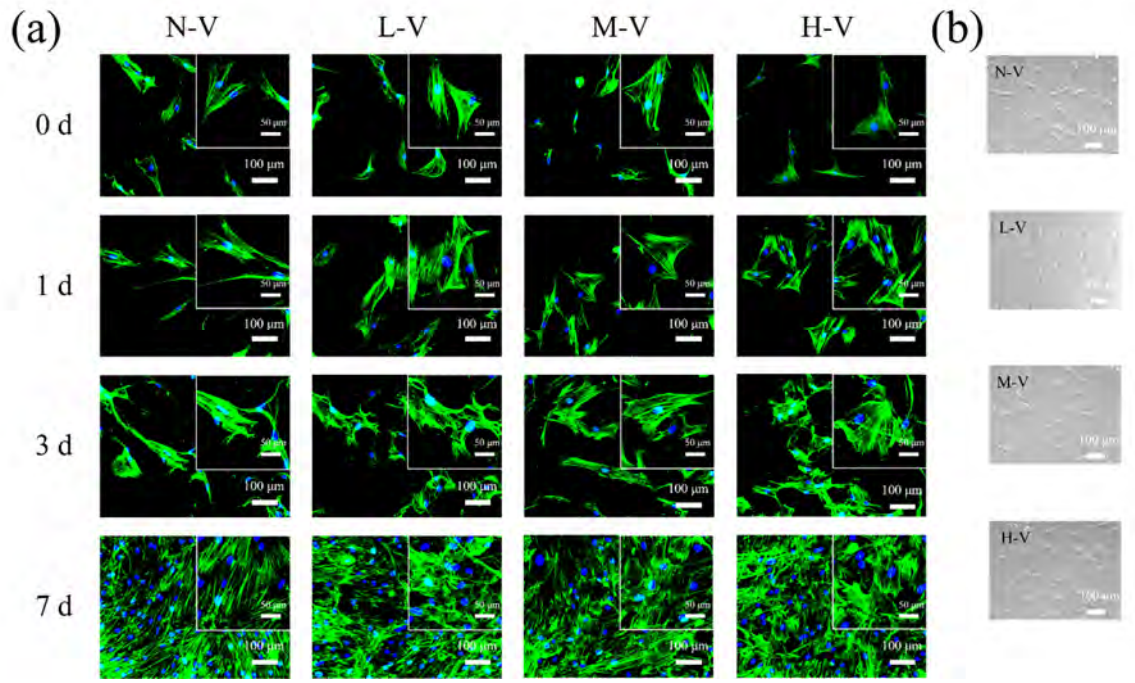

Figure S4. Morphology changes of hMSCs exposed to different viscous media under osteogenic differentiation. (a) F-actin staining of hMSCs under different viscosity exposure during osteogenic differentiation on 0, 1, 3 and 7 d. (b) Phase-contrast photomicrographs of hMSCs exposed to different viscous osteogenic induction media for 3 d.

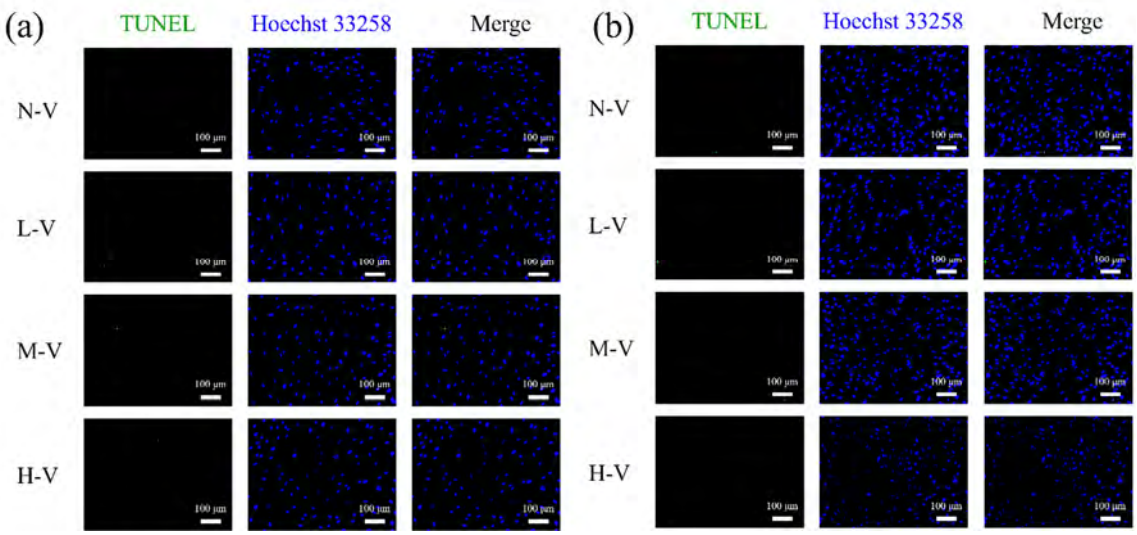

Figure S5. Apoptosis staining of hMSCs cultured in adipogenic viscous media (a) and osteogenic viscous media (b) for 7 d. Scale bar = 100 μm.

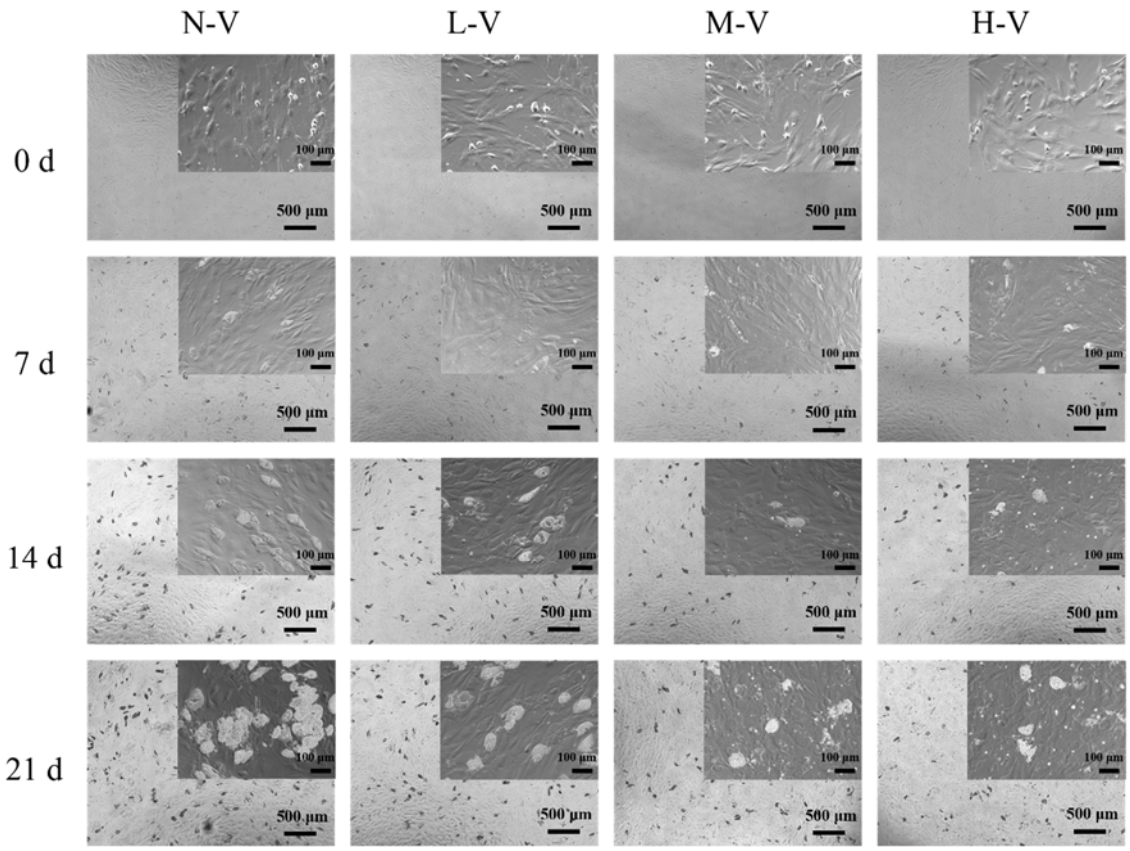

Figure S6. Phase-contrast photomicrographs of hMSCs exposed to different viscous media under adipogenic differentiation on 0, 7, 14 and 21 d. Scale bar = 500 μm, inserted scale bar = 100 μm.

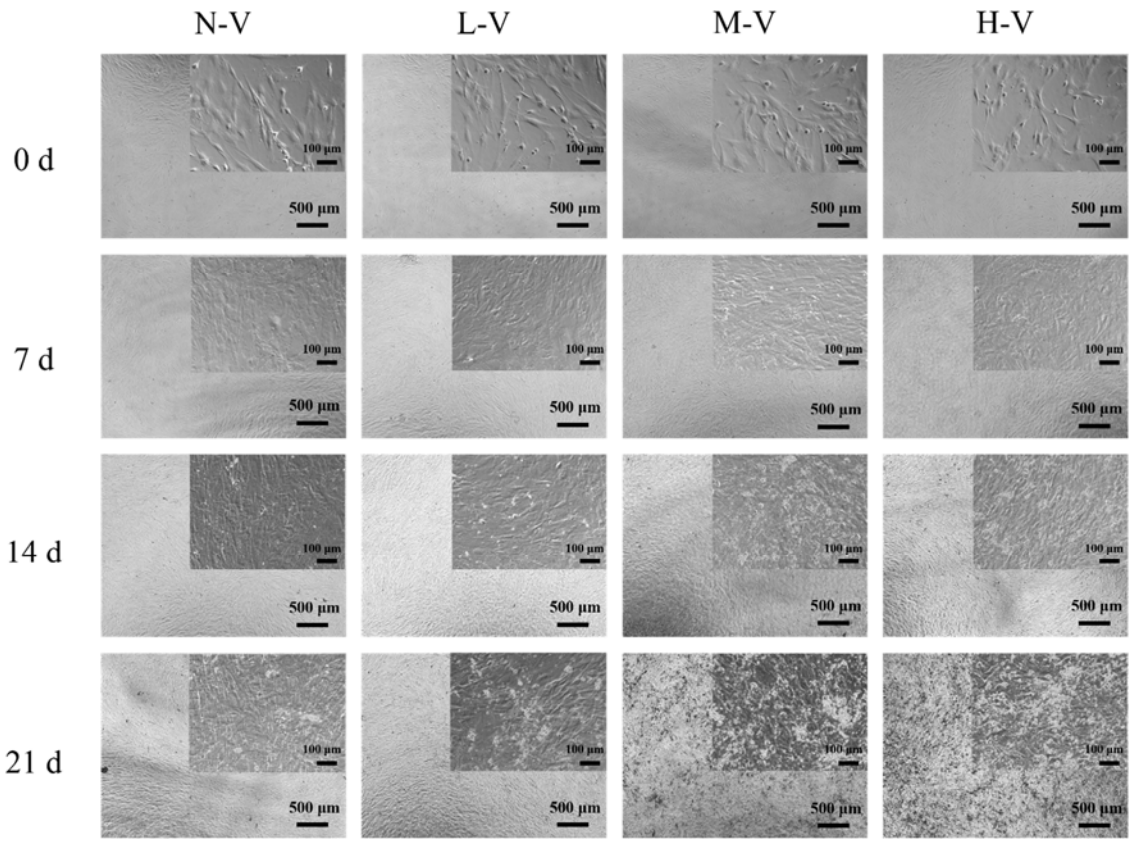

Figure S7. Phase-contrast photomicrographs of hMSCs exposed to different viscous media under osteogenic differentiation on 0, 7, 14 and 21 d. Scale bar = 500 μm, inserted scale bar = 100 μm.

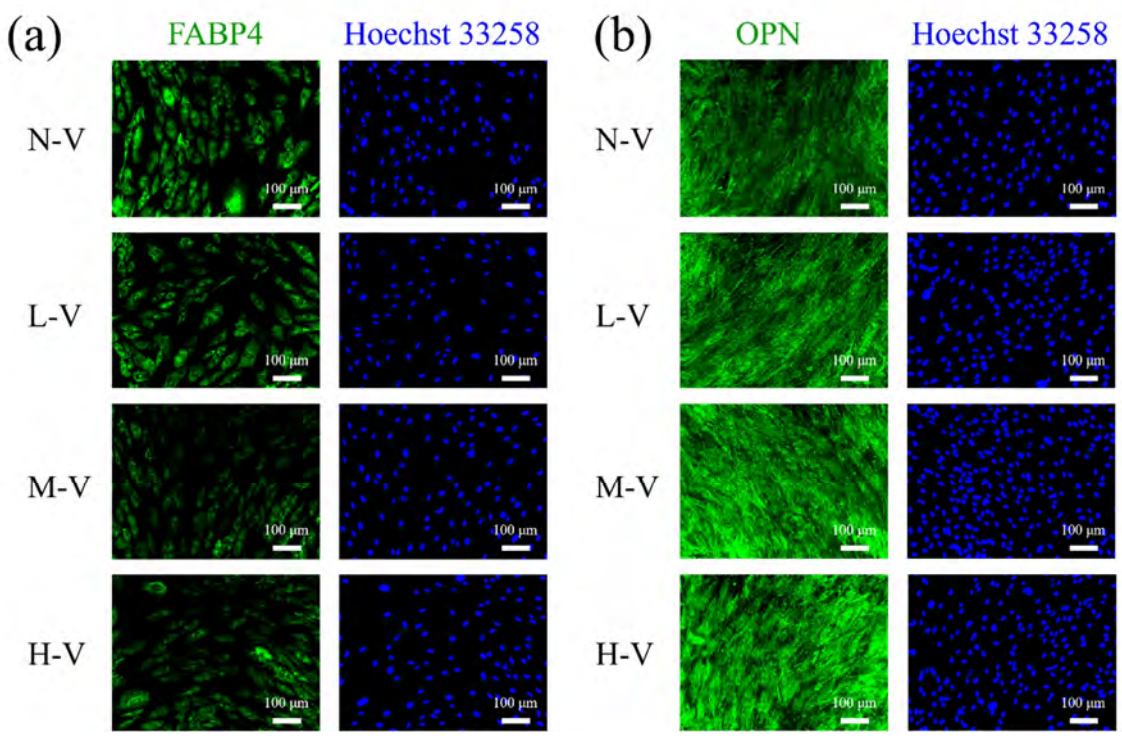

Figure S8. Immunofluorescence staining of FABP4 (a) and OPN (b) for adipogenic and osteogenic differentiation under different viscosity stimuli for 3 d, respectively. Cell nuclei were stained blue, scale bar = 100 μm.